Twelfth Australasian Fluid Mechanics Conference
The University of Sydney, Australia 1995

PRESSURE - VELOCITY CORRELATIONS IN SWIRLING PIPE FLOW

Anthony R. deL. Musgrove
12 Kelton Pl., Engadine
Sydney, N.S.W.
Australia

John D. Hooper
1 Blackbutt Pl., Engadine
Sydney, N.S.W.
Australia

Abstract

An improved frequency response, four-hole pressure probe (known as the Cobra probe) has been used to measure simultaneously the time dependent three orthogonal components of velocity and the mean and fluctuating components of static pressure in a swirling pipe flow. The flow was generated by a vane type swirler, and significant correlations between components of the turbulent velocity and the turbulent static pressure were shown to be present.

INTRODUCTION

The Cobra four-hole pressure probe is described in a separate paper in this conference (Hooper and Musgrove (1995)), which demonstrated the use of the probe to measure all components of the Reynolds stresses in developed single phase turbulent pipe flow, a calibration flow. The probe simultaneously resolves the three orthogonal turbulent velocity components and the time dependent static pressure at a point in the flow. It has been shown by the above paper that for pipe flow the axial turbulent velocity component is highly anti-correlated with the local turbulent static pressure, with a correlation coefficient of approximately -0.5. The operation and limitations on the use of the probe in a highly turbulent flows is explored by this paper.

The intensity of the pressure fluctuations at a point in a flow field (Hinze (1971)) is given via the Poisson equation by a volume integration over the neighbouring regions of the instantaneous momentum fluctuations. Turbulent pressure fluctuations can be generated in two ways: by a interaction between turbulent eddies and the mean shear, and in an interaction of turbulence with itself (George et al (1984)). The first mechanism can be subdivided into components involving the second moment of velocities and terms involving the third moment. Each component has a different frequency spectrum and can be expected to be of importance in different parts of a complicated flow, and at different frequencies. For example, George et al (1984) show that the third moment is identically zero in isotropic turbulent flow.

The measurement of pressure-velocity correlations away from a wall surface is beset with experimental difficulties, chief among which is the need to correlate the outputs of two different measuring devices at the same point in the flow. Nevertheless, Komerath et al (1985) and more recently Tsai et al (1993) have managed to show the importance of a static pressure correlation proportional to the product of the mean and turbulent stream velocities. This may correspond to the production of static pressure fluctuations via the turbulence-shear interaction.

In this paper experimental evidence is presented for a high correlation between selected components of the turbulent velocities and the turbulent static pressure, correlations that are significant in well defined regions of the flow field. It is shown that in the core region of the swirling flow where the reliability of the experimental data is considered to be high, the axial and tangential turbulent velocity components have a large anti-correlation with the turbulent static pressure field. For the central wake region of the flow, where the accuracy of the data is considerably reduced, there are indications of a large positive correlation between the radial turbulent velocity component and the turbulent static pressure. The peak values of this correlation occur in very high shear regions of the flow, and may be associated with the production of turbulence in these regions.

EXPERIMENTAL RIG

The experimental duct was a 140 mm i.d. pipe, 18 m long, with a two radial section guide vane swirler mounted on a 50 mm diameter pipe used to generate the tangential velocity component of the flow. The guide vane swirler was designed using blade element theory (Buckley et al, (1980)) to generate an equal magnitude of the axial and tangential velocity components at the pipe wall, with a forced vortex distribution for the tangential velocity elsewhere. The swirler had sixteen outer and eight inner vanes, and the 50 mm diameter pipe forming the hub was extended 160 mm downstream of the inner blades. The exit of the swirler was 0.58 m upstream of the pipe exit, and the measurement plane located 0.21 m or 1.5 pipe diameters upstream of this exit. The rig was operated by a single stage centrifugal fan blower driven by a 22 kW variable speed induction motor drive.

The Cobra probe was mounted on a computer driven radial traverse system which also had 360 degrees of rotation in the yaw plane of the probe. An automatic search routine, using sixteen equal increments in yaw, was used to locate the yaw angle at which the probe centre hole pressure was a maximum. Then ensembles of data, 20 record lengths long, were recorded by the 486 PC computer at this yaw angle. The digitisation frequency was 5.0 kHz and the record length was 4096, giving a total sampling time of just over sixteen seconds. A six pole, active, low pass filter with a 3 dB point set at 1.5 kHz was used with each of the four pressure signals to prevent aliasing of these signals. Approximately five minutes of computing time were needed to position the probe, record the data, and to compute the required mean and turbulent flow parameters at each radial position.

Experimental Results

The mean velocity distribution 2.5 pipe diameters downstream of the swirler is shown by figure 1.

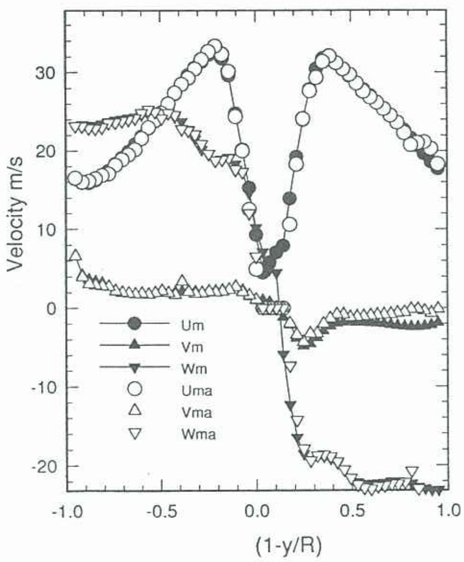

Mean Velocity Components

Figure 1

The axial radial and tangential mean velocity components Um, Vm and Wm are calculated from the average of the time records of the associated velocity components. Assuming that all the pressure data, corrected for the distortion introduced by the probe head to remote transducer transmission path (Hooper and Musgrove (1995)), generated data from the four calibration surfaces, each velocity mean is the average of approximately eighty two thousand individual estimates. The velocity vector must remain within the acceptance cone angle of the probe (within + and - 45 degrees in pitch and yaw angle), for the non-dimensional pressure ratios $X1$ and $X2$ (Hooper and Musgrove (1991)) to remain within the bounds of the calibration surfaces for total pressure, dynamic pressure, yaw and pitch angle. As will be shown subsequently, this condition was satisfied for the core region of the swirling flow.

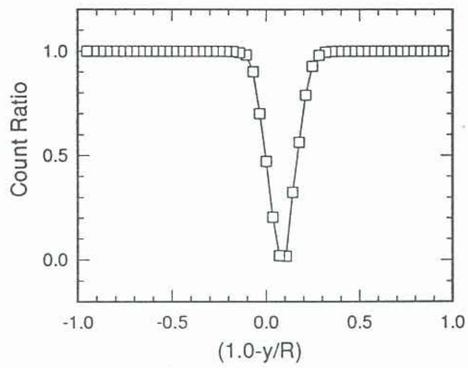

Count Ratio

Figure 2

The conventional method of calculating the mean velocity vector and static pressure is to simply average the four probe pressures, and to apply the ratios $X1$ and $X2$ derived from these averaged pressures to the calibration surfaces. This is in effect what is done by a low frequency response pressure probe, which in disregarding the effect of the turbulence intensity on the measured average pressure, measures effectively an R.M.S. velocity. The mean velocity estimates as a result of averaging the probe pressure records (Uma, Vma and Wma) are also shown by figure 1, and it is seen that the match between the two estimates is remarkably good for all components in this flow. The data for the axial and tangential components are almost coincident for the whole traverse. In highly turbulent flows, it is possible to have parts of the pressure time series generate velocity data from the calibration surfaces, but the mean pressure estimates to be off the calibration surfaces. Such data may show that the probe is not aligned with the mean velocity vector.

The flow field is seen to be slightly miss-aligned with the axis of the pipe, and the wake region generated by the 50 mm diameter stub axle of the swirler to extend between dimensionless wall distances between -0.2 to 0.2.

An experimental test of the data is simply to record the count ratio, or the number of pressure ratios that return data from the calibration surfaces, as a function of the record length. The count ratio data for this flow is shown by figure 2. The value for dimensionless wall distances greater in magnitude than 0.2 is high (effectively 1.0), and this region of the flow is considered to be the swirling core region of the flow. The turbulence intensity here is approximately 30%. The wake region shows a rapidly falling value of the count ratio, and for very low values ($0.0 < (1.0 - y/R) < 0.1$), the data is considered to be unreliable. This may be due to the low mean velocity in this region, with the difference between the local dynamic and static pressures beyond the resolution of the pressure transducers. Additionally, the time dependent velocity vector may not be within the acceptance cone angle of the probe for most of the time record.

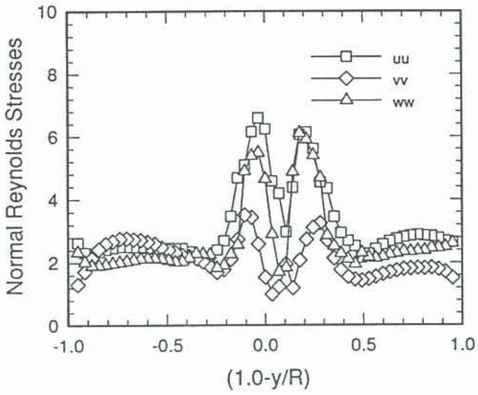

Normal Reynolds Stresses

Figure 3

The normal Reynolds stresses, divided by the pipe wall shear stress upstream of the swirler, are shown by figure 3. The wake region of the flow is highly turbulent, and the apparent reduction in the magnitude of these components in the centre of the wake is may be due to the very poor count ratio here.

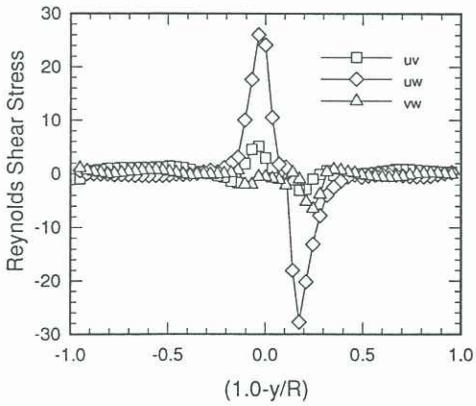

Reynolds Shear Stresses

Figure 4

The Reynolds shear stresses are shown by figure 4, and it is apparent that the interaction of the swirling outer flow region with the wake produces very high levels of the $-\rho\overline{uw}$ component of the shear stresses. The peak values of this variable occur just outside the low confidence region for the data. The same skew symmetric behaviour is present for $-\rho\overline{uv}$, although at a reduced magnitude.

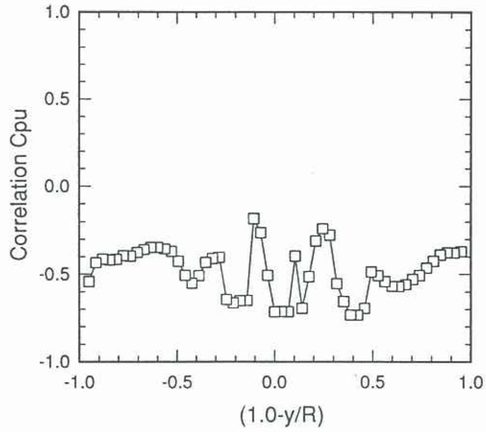

Correlation Cpu

Figure 5

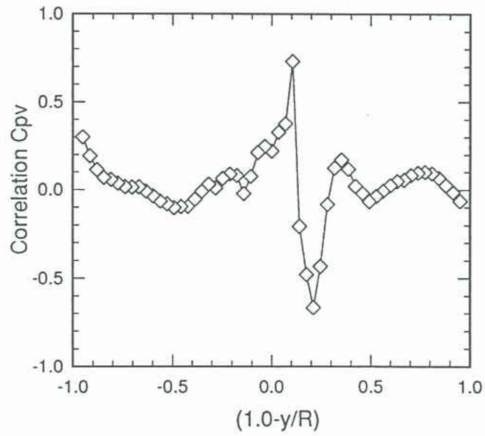

Correlation Cpv

Figure 6

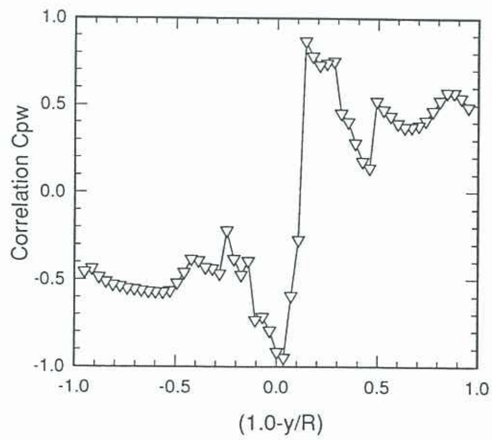

Correlation Cpw

Figure 7

The correlations between the turbulent velocity components and the turbulent static pressure field are shown by figures 5, 6 and 7 for Cpu, Cpv and Cpw.The anti-correlation between the turbulent axial velocity and pressure, figure 5, shows a similar value to the data for pipe flow when outside the wake region. The correlation between the radial turbulent velocity and the turbulent static pressure, figure 6, shows this to be generally of a relatively low magnitude. In the wake region, however, a strong positive correlation is shown, although these large values are present immediately adjacent to the region of low count ratio. The corresponding figure 7 for the tangential turbulent velocity component and turbulent static pressure field shows the same large anti-correlation between these variables for the whole of the flow field . Remarkably high values of this anti-correlation are reached within the wake region, although the reliability of the data for this region is below that for the swirling outer core of the flow.

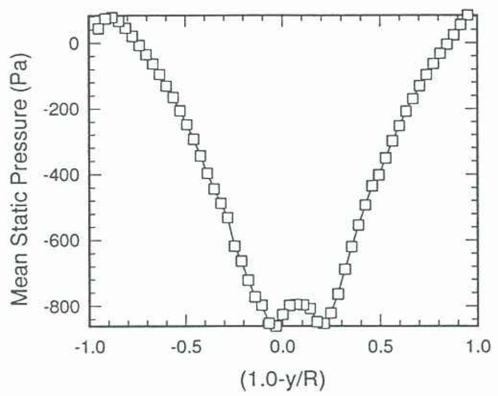

Mean Static Pressure

Figure 8

The mean static pressure distribution down stream of the swirler is shown by figure 8. The apparent though small static pressure recovery in the centre of the wake may be due to the poor count ratio here. However, in previous studies of swirled flow in a symmetrical annulus, the values of the static pressure at the inner and outer duct walls have been compared to the probe values, with a good agreement between these estimates. This earlier confirmation of the operation of the probe leads weight to the static pressure distribution shown by figure 8.

Conclusion

Significant correlations between all turbulent velocity components and the turbulent static pressure have been shown by the data presented for swirling pipe flow. Although the interpretation of this data is not clear at this time, the probe represents a new technique for making these difficult and largely unreported measurements. The ability of the Cobra pressure probe to reproduce the Reynolds stress distribution in a calibration pipe flow substantiates the measurement technique.

REFERENCES

Buckley, P.L., Craig, D., Davis, L. and Schwartzkopf, K.G. 1980, AA/SAE/ASME Joint Propulsion Conf. AIAA-80-1119

George, W.K., Thom, A.S. and Yang, A.D. 1984 J. Fluid Mech., 148, p155

Hinze, J.O. "Turbulence", McGraw-Hill, 1975, p305

Hooper , J.D and Musgrove, A.R. deL, 1995 Twelth Aust. Fluid Mech. Conf.

Hooper, J.D. and Musgrove, A.R. deL, 1991 Proc. 4th Int. Symp. on Transport Phenomenon in Heat and Mass Transfer, U. of N.S.W., p1364

Komerath, N.M., Hegde, U.G. and Stahle, W.C., 1985 AIAA Journal, 23, p1320

Tsai, G. L and Yang, J.T. 1993 Exp. in Fluids 15, p462

Acknowledgement

The experiments described here were performed by the while the authors were employed by the CSIRO Division of Minerals. The technical assistance of Mr Stephen Rainey was greatly appreciated.